JACS
JOURNAL OF THE AMERICAN CHEMICAL SOCIETY
Article
Cite This: J. Am. Chem. Soc. 2020, 142, 283−289
pubs.acs.org/JACS

Block Copolymer Vitrimers

Jacob J. Lessard,[†] Georg M. Scheutz,[†] Seung Hyun Sung,[‡] Kayla A. Lantz,[‡] Thomas H. Epps, III,[*,‡,§] and Brent S. Sumerlin[*,†]

[†]George and Josephine Butler Polymer Research Laboratory, Center of Macromolecular Science, Department of Chemistry, University of Florida, Gainesville, Florida 32611, United States

[‡]Center for Research in Soft matter & Polymers, Department of Chemical & Biomolecular Engineering, University of Delaware, Newark, Delaware 19716, United States

[§]Department of Materials Science and Engineering, University of Delaware, Newark, Delaware 19716, United States

Supporting Information

ABSTRACT: In this report, we merge block copolymers with vitrimers in an effort to realize the prospect of higher-order, nanoscale control over associative cross-link exchange and flow. We show the use of controlled polymerization as a vital tool to understand fundamental structure−property effects through the precise control of polymer architecture and molecular weight. Vitrimers derived from self-assembling block copolymers exhibit superior resistance to macroscopic deformation in comparison to their analogs generated from statistical copolymers. Our results suggest that the enhanced creep resistance achieved by control over chain topology in block vitrimers can be used to tune viscoelastic properties. The resistance to macroscopic deformation that arises from a microphase-separated structure in this new class of materials differentiates block vitrimers from their statistical counterparts and introduces the potential of topology-control over viscoelastic flow.

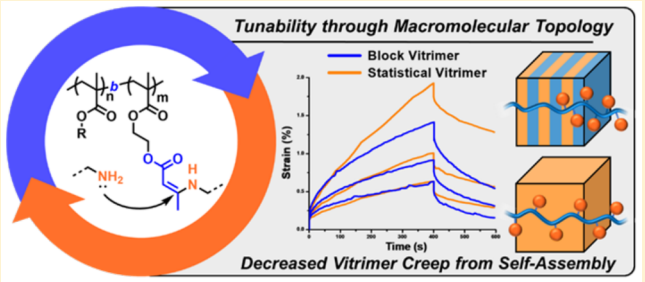

INTRODUCTION

Direct mechanical reprocessing is a promising avenue for repurposing polymer materials. However, covalently cross-linked thermosets, often employed due to their enhanced thermal, mechanical, and chemical resistance, feature a permanent network structure that complicates most recycling and reprocessing approaches.[1] Recent advances have been made to impart reprocessability into covalent network materials through the incorporation of reversible cross-links.[2,3] Such covalent adaptable networks (CANs) rely on dynamic cross-links that reversibly exchange to permit reprocessability.[4−9] In particular, thermally activated associative CANs, or vitrimers,[10,11] have shown great promise for the development of recyclable thermosets.[12] The associative bond exchange in vitrimers leads to networks with a constant cross-link density at all temperatures and combines the pliability of thermoplastics with the robust thermomechanical and chemical resistant behavior of thermosets. Exchange chemistries such as transesterification,[13−17] amine exchange of vinylogous urethanes,[18−22] thiol exchange,[23] silyl ether transalkoxylation,[24,25] diketoenamine exchange,[26] olefin metathesis,[27] and dioxaborolane metathesis[28,29] have been proposed for such processable thermosets.

Tuning the thermal response, and consequently the range of service and processing temperatures of vitrimers, has been achieved through variation of network components,[30,31] catalysts,[11] or exchange chemistries.[32] However, few examples have exploited the potential of predesigned, hierarchical organization of network elements in vitrimers,[22,29,33,34] and very little is known about the effect of this approach on material properties. In one example, Leibler and co-workers demonstrated that incompatibility between the various components in a vitrimer system resulted in higher-order assemblies through the clustering of dioxaborolane maleimide cross-links in a polyethylene vitrimer matrix.[29] These effects were hypothesized to yield an increased rate of flow for these networks; however, a specific comparison of self-assembled and non-assembled vitrimers has yet to be undertaken.

To understand how controlling polymer architecture and inducing microphase separation impact viscoelasticity, well-defined statistical copolymers and block copolymers were generated and cross-linked with a bis-functional amine to form vinylogous urethane (VU) vitrimers.[20] We hypothesized that changing the polymer architecture from a linear, statistical copolymer, with homogeneously dispersed VU cross-links throughout the network, to a linear, block copolymer, with locally concentrated and spatially segregated VU moieties, would lead to dramatically different vitrimer network structures and confinement of cross-link exchange. Specifically, we reasoned that microphase separation arising from immiscibility between polymer blocks comprised of butyl methacrylate

Received: September 30, 2019
Published: December 3, 2019

DOI: 10.1021/jacs.9b10360
J. Am. Chem. Soc. 2020, 142, 283−289

(BMA) and 2-acetoacetoxyethyl methacrylate (AAEMA) will alter the diffusion of polymer chains and the exchange of cross-links to ultimately impart topology-control over vitrimer material properties (Figure 1).

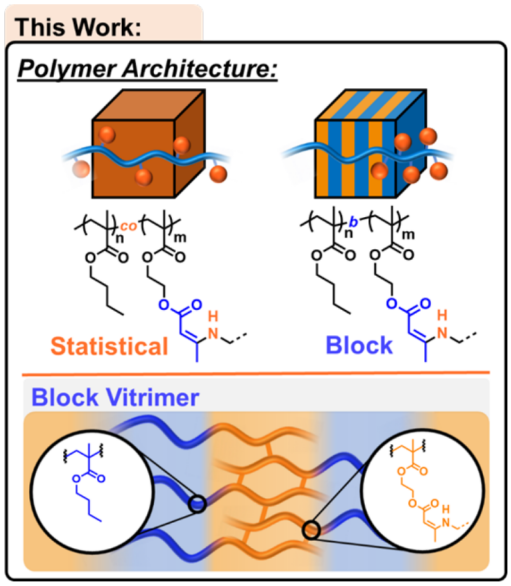

Figure 1. Depiction of statistical and block vitrimers derived from butyl methacrylate and 2-acetoacetoxyethyl methacrylate (top); envisioned microphase separation of block vitrimers (bottom).

RESULTS AND DISCUSSION

To investigate the impact of polymer architecture on vitrimer material properties, we employed reversible addition–fragmentation chain transfer (RAFT) polymerization of BMA and AAEMA to generate statistical copolymers (P(BMA-*co*-AAEMA)) and block copolymers (PBMA-*b*-PAAEMA) of similar molecular weight and composition (1:1 molar ratio of BMA to AAEMA) (Figures 2 and S1–S17). Importantly, RAFT polymerization enables control over polymer architecture and molecular weight and is an exceptionally well-suited platform for the synthesis of vinyl-derived vitrimer systems with topological variations.[35,36] AAEMA, the *β*-ketoester-bearing repeat units, serve as reactive handles for facile downstream cross-linking via VU formation with primary amines, while the BMA repeat units remain inert to the exchange process.[18,19,22,37]

The polymerization kinetics for the statistical copolymerization were investigated to verify random incorporation of the monomers. ^{1}H NMR spectroscopy revealed that the molar ratio of unreacted AAEMA to BMA remained constant throughout the polymerization, suggesting that the monomers were incorporated at similar rates and were evenly dispersed throughout the chain (Figure 2A). Characterization of the polymers via gel permeation chromatography (GPC) revealed a uniform shift of molecular weight during the polymerization, low dispersity polymers, and relative agreement between the experimental and theoretical molecular weights, all of which indicated a well-controlled polymerization (Figures 2B and S1 and S2).

For the formation of the block copolymer, a PBMA (7.4 kg/mol) macro-chain-transfer agent was chain-extended with AAEMA to yield a block copolymer with the same total AAEMA incorporation as the statistical copolymer (50 mol % AAEMA) (Figure 2C). Both the statistical and block copolymers were subjected to excess azobis(isobutyronitrile) initiator in the absence of monomer to replace the RAFT trithiocarbonate end-groups with 2-cyanopropyl moieties,[38] thereby preventing the potential for side reactions during network formation with the amine cross-linker.[20,37] Successful

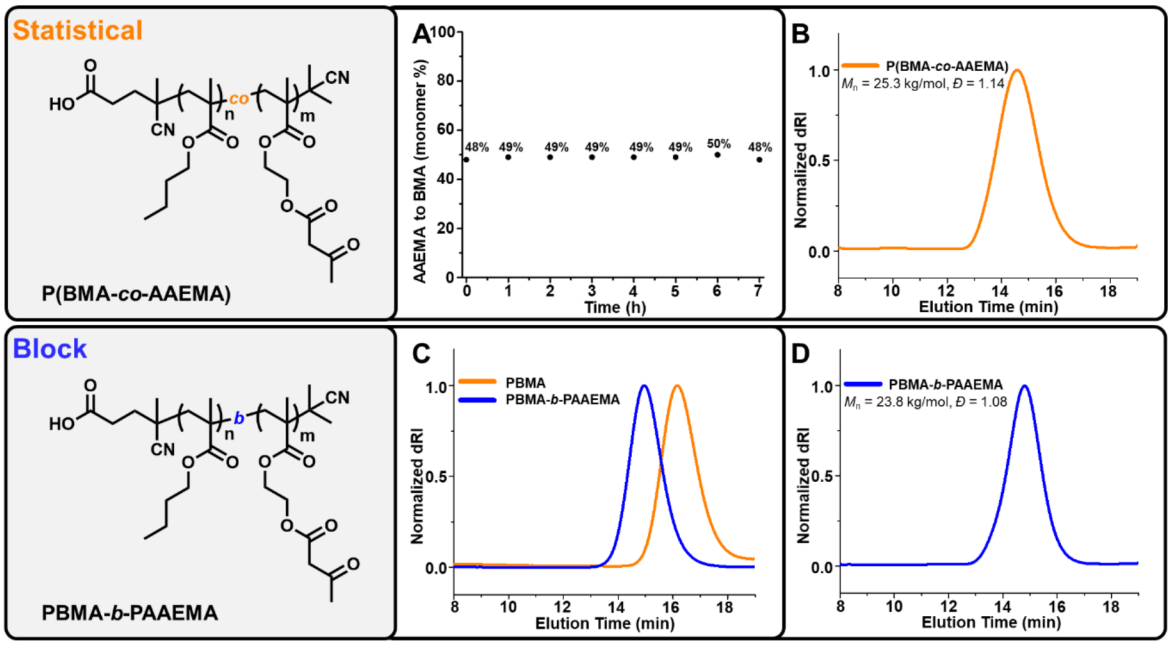

Figure 2. Statistical and block copolymer synthesis. (A) Ratio of unreacted AAEMA to BMA throughout the polymerization, indicating proportional and statistical incorporation of each comonomer into the polymer. (B) GPC trace of P(BMA-*co*-AAEMA) with the number-average molecular weight (M_n) and dispersity ($Đ$) after end-group removal. (C) GPC trace of PBMA (orange) and PBMA-*b*-PAAEMA (blue). (D) GPC trace of PBMA-*b*-PAAEMA after end-group removal.

DOI: 10.1021/jacs.9b10360
J. Am. Chem. Soc. 2020, 142, 283–289

end-group removal was confirmed during GPC analysis with a UV−vis detector by the disappearance of the absorption band at 365 nm, corresponding to the $\pi \rightarrow \pi^*$ electronic transition of the trithiocarbonate (Figure S10, S14, and S15). The statistical copolymer (M_n = 25.3 kg/mol after end-group removal) and the block copolymer (M_n = 23.8 kg/mol after end-group removal) were both shown to retain the β-ketoester functional group via NMR and Raman spectroscopy (Figures S3−S7, S16, and S17). Importantly, both the molecular weights and AAEMA incorporation of the statistical copolymer and block copolymer were very similar, which suggests any differences in material properties should arise only from differences in hierarchical assembly.

With the copolymers in hand, statistical vitrimers and block vitrimers were formed by solution casting each copolymer with xylylene diamine cross-linker (0.9 equiv to AAEMA units) from THF (Figures S18 and S19). After solvent evaporation at room temperature, the resulting organogels were cured at 80 °C under reduced pressure to produce cross-linked films (Figure S18A−C and S19A−C). The films were ground and compression molded into disks or bars at 160 °C under reduced pressure and analyzed (Figure 3, S18D−F, S19D−F, and S20−23).

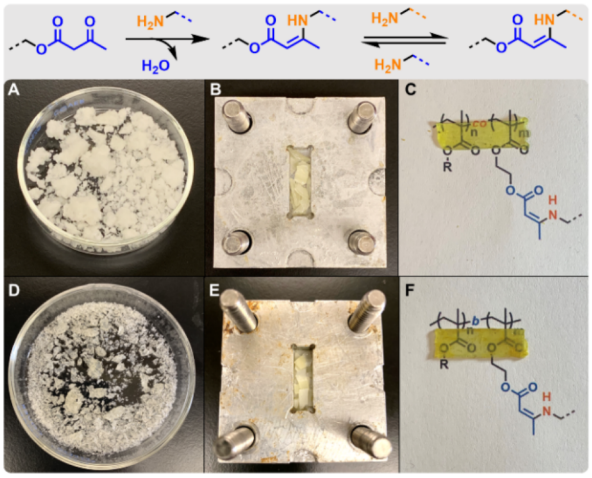

Figure 3. Vitrimer synthesis and processing. (A) P(BMA-*co*-AAEMA) before cross-linking. (B) Statistical vitrimer after curing at 80 °C and before processing in a compression mold. (C) Statistical vitrimer after processing at 160 °C. (D) PBMA-*b*-PAAEMA before cross-linking. (E) Block vitrimer after curing at 80 °C and before processing. (F) Block vitrimer after processing at 160 °C.

We probed the reprocessability of each system by two additional destruction-compression cycles (Figure 4). Using ATR-FTIR spectroscopy, optical microscopy coupled with Raman spectroscopy, differential scanning calorimetry (DSC), dynamic mechanical analysis (DMA), and solubility studies, the retention of chemical and mechanical properties of the (re)processed vitrimers was assessed (Figures 4and S24−S35). We detected no change in the IR absorbance or Raman signal of the VU moiety over all reprocessing cycles (Figures S24−S30). The constant glass transition temperature (T_g) obtained from DSC after multiple cycles and an unaltered rubbery plateau of the storage modulus from DMA after each destruction-compression sequence indicated retention of the vitrimer network integrity (Figure S32−S34).[39,40]

We noted a single T_g around 82 °C for the statistical vitrimer. The block copolymer demonstrated a clear T_g transition at 110 °C (Figure 4), which arises from the AAEMA block, and the first derivative of the DSC thermogram offered evidence of a second T_g at 34 °C, which we attribute to the BMA block (Figure S31). The presence of two transitions can correspond to a microphase-separated structure.[41] Additionally, we found further evidence of microphase separation in the tan(δ) plots, obtained from DMA, from the pronounced shoulder at lower temperatures for the block vitrimers that was not apparent in the statistical specimens (Figure S34). In all cases, there was no significant change in the T_g values of the block vitrimers across heating/cooling and (re)processing cycles.

To verify microphase-separation in the block vitrimers, we analyzed the bulk and thin film behavior of the polymer systems. Bulk samples, generated as described in the Supporting Information, were probed via small-angle X-ray scattering (SAXS). Data for the uncross-linked block copolymers showed reflections corresponding to q*, 2q*, and 3q*, suggesting a lamellar morphology with a domain spacing of 17−18 nm; no reflections were noted for the statistical copolymer, suggesting a disordered morphology with minimal microphase separation (Figure 5A). Importantly, we observed no order−disorder transition temperature (T_{ODT}) for the block copolymers over the probed temperature range (60−180 °C), which indicates that microphase separation for the block copolymer assembly persists over the entire temperature range considered (Figure S48). The block copolymer was then infused with xylylene diamine cross-linker and analyzed via SAXS during a temperature ramp from 60−180 °C. These data indicated that the self-assembled structure remains intact and with similar characteristic feature sizes following cross-linking (Figures 5B and S49). To further demonstrate the versatility and potential utility of these self-assembling copolymer vitrimers, the thin film behavior of the materials was assessed via atomic force microscopy (AFM).

Using flow coating from THF, both statistical and block copolymers were cast to ∼30−60 nm film thickness. Microphase separation of the block copolymer was revealed by AFM, while no microphase separation was found for the statistical copolymer prior to annealing (Figure S37−S39). Both thermal and solvent vapor annealing (SVA) of the thin films resulted in ordered lamellae for the block copolymer samples and an absence of visual features for statistical copolymer specimens. To determine the effect of cross-linking on self-assembly, the thin-films were annealed for 8 h at 80 °C under xylylene diamine vapor (Figure S40−S46). Notably, the lamellae persisted in the block vitrimer films, while the statistical vitrimer films still led to featureless AFM images (Figure 5C,D). To confirm successful cross-linking of the self-assembled thin film structures, we washed the vapor-annealed thin-films with THF, and no dissolution of the materials was observed, consistent with the films having been cross-linked (Figure 5E). Finally, the incorporation of the cross-linker was further confirmed through scanning electron microscopy (SEM) coupled with an energy dispersive X-ray (EDX) analyzer, which provides identification of the elemental composition for the sample, showing distinct signals for nitrogen stemming from the diamine cross-linker dispersed throughout the sample (Figures 5F and S47). Additionally, we determined the total amine content relative to polymer in the thin films by X-ray photoelectron spectroscopy (XPS), offering

DOI: 10.1021/jacs.9b10360
J. Am. Chem. Soc. 2020, 142, 283−289

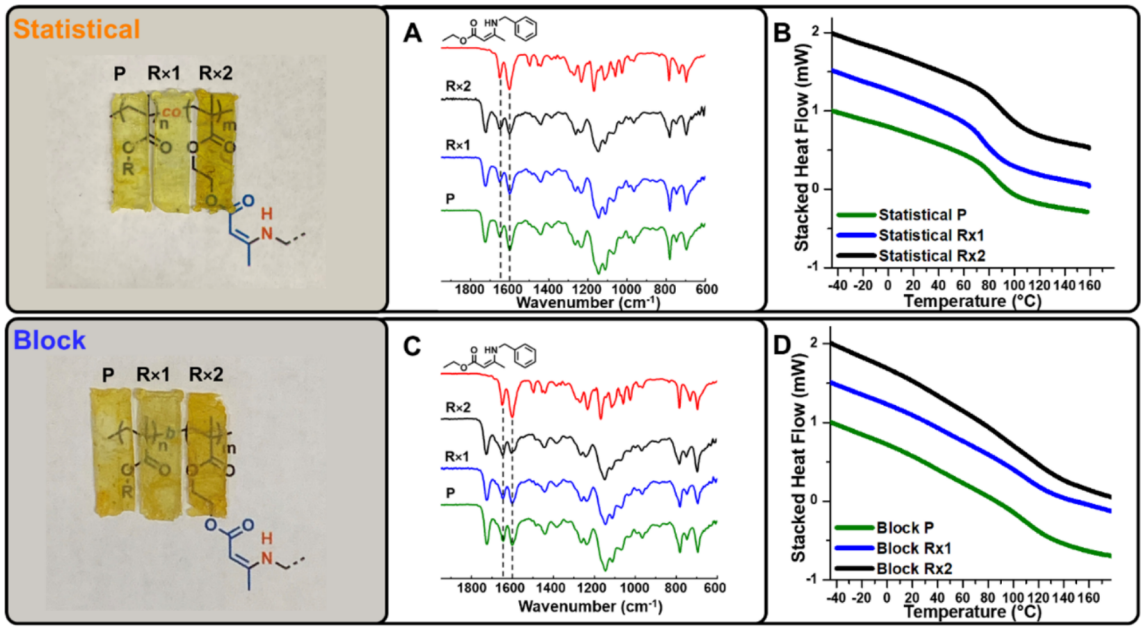

Figure 4. Reprocessing cycles of statistical and block vitrimers. (A) ATR-FTIR spectra of the statistical vitrimer after (re)processing cycles and the model VU compound ethyl-3-(benzylamino)-2-butenoate. (B) DSC of the statistical vitrimer after (re)processing cycles (heating, exotherm up). (C) ATR-FTIR spectra of the block vitrimer after (re)processing cycles and the model VU compound. (D) DSC of the block vitrimer after (re)processing cycles (heating, exotherm up).

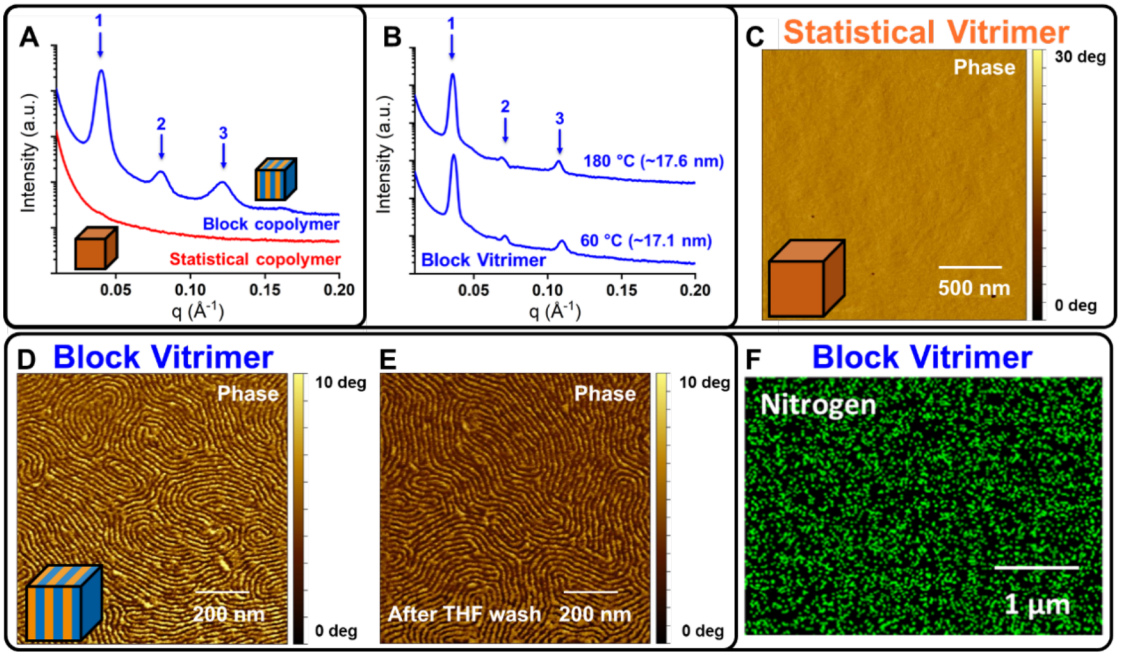

Figure 5. Thin-film studies of vitrimer networks. (A) SAXS profile of bulk statistical (red) and block (blue) copolymers, showing self-assembly and domain spacing of the block copolymer. (B) SAXS profile of bulk block vitrimer heated to 60 and 180 °C in the SAXS instrument, showing the retention of self-assembled morphology over the probed temperature range. (C) AFM image of the statistical vitrimer thin-film after annealing and cross-linking. (D) AFM image of thin films of the block vitrimer after solvent vapor annealing and cross-linking, confirming microphase-separation. (E) AFM image of thin films of the block vitrimer after washing with THF, confirming no dissolution of the cross-linked network and retention of the self-assembled morphology. (F) SEM-EDX image of the block vitrimer after solvent vapor annealing (SVA) and cross-linking, verifying incorporation of amine cross-links from nitrogen signals.

evidence of approximately one free amine per cross-link, indicating there were excess amines present in the film to effect the exchange needed for vitrimeric behavior. (Figures S51 and S52 and Table S1).[20] Lastly, self-assembly of the block vitrimers via solution casting into thin films resulted in lamellar structures observed by AFM with domain sizes of 16.0−16.5 nm. These sizes are comparable to those calculated from SAXS analyses (~17 nm) of the bulk samples after thermal annealing. Thus, the microphase separation of the block vitrimers is suited for both bulk and thin film materials applications.

To investigate the differences in flow behavior between the statistical and block vitrimers, we carried out stress-relaxation

DOI: 10.1021/jacs.9b10360
J. Am. Chem. Soc. 2020, 142, 283−289

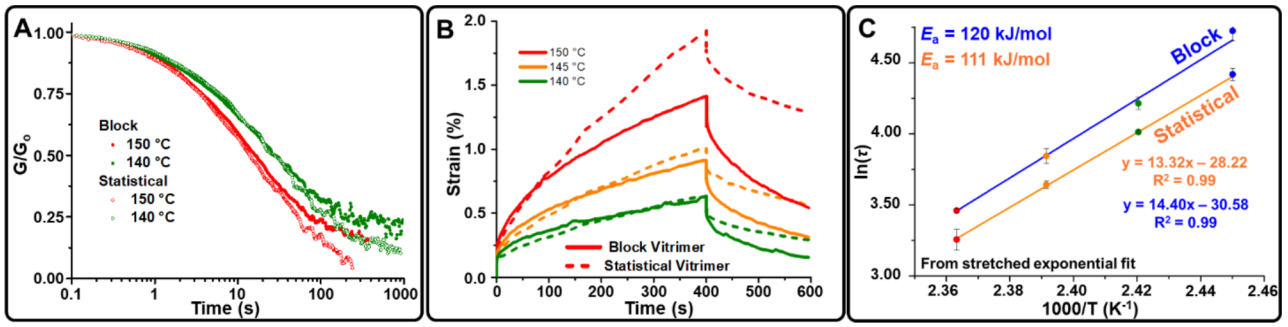

Figure 6. Rheology of block and statistical vitrimers. (A) Overlay of statistical and block vitrimer stress relaxation at 140 and 150 °C at a constant 0.3% strain. (B) Overlay of statistical and block vitrimer creep recovery at 140, 145, and 150 °C at a constant stress of 5000 Pa. (C) Arrhenius plot of statistical and block vitrimers, with activation energies (E_a), where τ was obtained from a stretched exponential fit of the stress relaxation.

and creep-recovery experiments for each (Figures 6 and S53–S63). The stress relaxation of the statistical and the block vitrimer were very similar at time scales shorter than 100 s (Figure 6A). However, we found significant deviation at longer time scales (>100 s). While the statistical vitrimer was able to fully relax the exerted stress within 1000 s, the block vitrimer transitioned into much slower modes of stress relaxation, with a portion of the stress being retained after a similar time. This deviation in flow behavior at longer time scales also was reflected in the creep recovery results (Figure 6B), where at 150 °C, the creep of the statistical and the block vitrimer was very similar up to 100 s and a strain of 0.75%. However, at longer time scales and strains above 0.75% (i.e., at greater deformations), the statistical vitrimer crept 37% more than the block vitrimer. Furthermore, the block vitrimer recovered strain to a much greater extent (88% more than the statistical vitrimer at 150 °C), indicating that less permanent deformation had occurred. We attribute the resistance to macroscopic deformation in the block vitrimer to the microphase-separated network structure that results in a higher local cross-link structure and restricts network strand diffusion.

Finally, we aimed to investigate the temperature-dependent flow of statistical and block vitrimers by determining the energy of activation for viscous flow (E_a). E_a can be obtained from the slope of the Arrhenius plot of the characteristic relaxation time (τ) versus temperature and can be interpreted as the sensitivity of viscous flow to temperature. Often, τ is identified as the time when the normalized stress in stress relaxation experiments approaches the value of 1/e (Figures S56A, S57A, and S58–S59).[13,42] However, this model is only valid for stress relaxation following a single Maxwell element,[42] which is not the case for these statistical and block vitrimers, as evidenced by the fact that the stress relaxation curves of neither vitrimer could be fit to a single Maxwell relaxation mode. Therefore, a stretched exponential decay, which accounts for multiple modes of relaxation,[16,43] was employed to determine τ at each temperature (Tables S2–S3 and Figures S56B and S57B). The Arrhenius plots were linear for both vitrimers over the probed temperature range, and E_a was found to be 111 ± 7 kJ/mol for the statistical vitrimer and 120 ± 6 kJ/mol for the block vitrimer (Figure 6C). It is important to note that this difference in E_a is solely due to the different architectures of the two networks, as the exchange chemistry, the molecular weight, and the cross-linker content were equal for both vitrimers. The higher E_a of the block vitrimer indicates that viscous flow of this material changed more dramatically with temperature than the statistical vitrimer with lower E_a. Investigations about the consequences of network structure in relation to E_a and long-term viscous flow are a subject of ongoing research efforts.

CONCLUSION

Until now, block copolymers have not been employed to investigate the concept of topology-control and microphase separation in associatively cross-linked networks. In our report, vitrimers from statistical and block copolymers were synthesized and analyzed in terms of chemical, thermal, and mechanical properties. The precursor polymers were obtained using RAFT polymerization, which enabled the generation of copolymers with similar molecular weights and cross-linker incorporation but different topologies. Both vitrimer systems exhibited excellent thermal reprocessability, with full retention of chemical and thermo-mechanical properties. Bulk and thin-film analysis of the block vitrimer revealed self-assembly into lamellae, while the statistical vitrimer exhibited a nonphase-separated morphology. Importantly, the block vitrimer displayed similar stress-relaxation and creep at short time scales and small deformations but drastically reduced macroscopic flow at longer time scales and larger deformations. We believe this resistance to macroscopic deformation for the block vitrimer is due to the microphase-separated network structure, which imposes additional constraints on network strand diffusion and a higher local cross-link concentration. This report is the first comprehensive investigation of topology-control in associatively cross-linked networks and introduces block copolymer self-assembly into the nascent field of vitrimers. On the basis of our findings, we believe that self-organization effects in vitrimer networks can be leveraged for further development of creep-resistant reprocessable materials.

ASSOCIATED CONTENT

Supporting Information

The Supporting Information is available free of charge at https://pubs.acs.org/doi/10.1021/jacs.9b10360.

Materials, instrumentation, polymer synthesis, polymer characterization, vitrimer synthesis, vitrimer characterization, vitrimer reprocessing, thin film studies, rheology, and vitrimer chemical recycling (PDF)

AUTHOR INFORMATION

Corresponding Authors

*thepps@udel.edu

*sumerlin@chem.ufl.edu

DOI: 10.1021/jacs.9b10360
J. Am. Chem. Soc. 2020, 142, 283–289

ORCID

Jacob J. Lessard: 0000-0003-2962-6472
Seung Hyun Sung: 0000-0002-7515-1183
Thomas H. Epps, III: 0000-0002-2513-0966
Brent S. Sumerlin: 0000-0001-5749-5444

Notes

The authors declare no competing financial interest.

■ ACKNOWLEDGMENTS

This material is based upon work supported by the National Science Foundation (NSF DMR-1904631). S.H.S. and T.H.E. thank (NSF DMR-1610134) for financial support for the film fabrication and characterization efforts. T.H.E. and S.H.S. also acknowledge the W.M. Keck Electron Microscopy Facility at the University of Delaware for the use of the AFM instrument, which is partially supported by the Delaware COBRE program with a grant from NIGMS (5 P30 GM110758-02) of the National Institutes of Health (NIH). T.H.E. and K.A.L. thank (NSF-1428149) for the use of the XPS instrument. The authors acknowledge Michael B. Sims for assistance with figure preparation.

■ REFERENCES

(1) Garcia, J. M.; Robertson, M. L. The future of plastics recycling. *Science* **2017**, *358*, 870−872.

(2) Fortman, D. J.; Brutman, J. P.; De Hoe, G. X.; Snyder, R. L.; Dichtel, W. R.; Hillmyer, M. A. Approaches to Sustainable and Continually Recyclable Cross-Linked Polymers. *ACS Sustainable Chem. Eng.* **2018**, *6*, 11145−11159.

(3) Sumerlin, B. S. Next-generation self-healing materials. *Science* **2018**, *362*, 150−151.

(4) Bowman, C. N.; Kloxin, C. J. Covalent Adaptable Networks: Reversible Bond Structures Incorporated in Polymer Networks. *Angew. Chem., Int. Ed.* **2012**, *51*, 4272−4274.

(5) Roy, N.; Bruchmann, B.; Lehn, J.-M. DYNAMERS: dynamic polymers as self-healing materials. *Chem. Soc. Rev.* **2015**, *44*, 3786−3807.

(6) Chen, X.; Dam, M. A.; Ono, K.; Mal, A.; Shen, H.; Nutt, S. R.; Sheran, K.; Wudl, F. A Thermally Re-mendable Cross-Linked Polymeric Material. *Science* **2002**, *295*, 1698−1702.

(7) Kloxin, C. J.; Bowman, C. N. Covalent adaptable networks: smart, reconfigurable and responsive network systems. *Chem. Soc. Rev.* **2013**, *42*, 7161−7173.

(8) Chakma, P.; Konkolewicz, D. Dynamic Covalent Bonds in Polymeric Materials. *Angew. Chem., Int. Ed.* **2019**, *58*, 9682−9695.

(9) Wojtecki, R. J.; Meador, M. A.; Rowan, S. J. Using the dynamic bond to access macroscopically responsive structurally dynamic polymers. *Nat. Mater.* **2011**, *10*, 14−27.

(10) Denissen, W.; Winne, J. M.; Du Prez, F. E. Vitrimers: permanent organic networks with glass-like fluidity. *Chem. Sci.* **2016**, *7*, 30−38.

(11) Capelot, M.; Unterlass, M. M.; Tournilhac, F.; Leibler, L. Catalytic Control of the Vitrimer Glass Transition. *ACS Macro Lett.* **2012**, *1*, 789−792.

(12) Scheutz, G. M.; Lessard, J. J.; Sims, M. B.; Sumerlin, B. S. Adaptable Crosslinks in Polymeric Materials: Resolving the Intersection of Thermoplastics and Thermosets. *J. Am. Chem. Soc.* **2019**, *141*, 16181−16196.

(13) Montarnal, D.; Capelot, M.; Tournilhac, F.; Leibler, L. Silica-Like Malleable Materials from Permanent Organic Networks. *Science* **2011**, *334*, 965−968.

(14) Capelot, M.; Montarnal, D.; Tournilhac, F.; Leibler, L. Metal-Catalyzed Transesterification for Healing and Assembling of Thermosets. *J. Am. Chem. Soc.* **2012**, *134*, 7664−7667.

(15) Snyder, R. L.; Fortman, D. J.; De Hoe, G. X.; Hillmyer, M. A.; Dichtel, W. R. Reprocessable Acid-Degradable Polycarbonate Vitrimers. *Macromolecules* **2018**, *51*, 389−397.

(16) Self, J. L.; Dolinski, N. D.; Zayas, M. S.; Read de Alaniz, J.; Bates, C. M. Brønsted-Acid-Catalyzed Exchange in Polyester Dynamic Covalent Networks. *ACS Macro Lett.* **2018**, *7*, 817−821.

(17) He, C.; Shi, S.; Wang, D.; Helms, B. A.; Russell, T. P. Poly(oxime−ester) Vitrimers with Catalyst-Free Bond Exchange. *J. Am. Chem. Soc.* **2019**, *141*, 13753−13757.

(18) Denissen, W.; Rivero, G.; Nicolaÿ, R.; Leibler, L.; Winne, J. M.; Du Prez, F. E. Vinylogous Urethane Vitrimers. *Adv. Funct. Mater.* **2015**, *25*, 2451−2457.

(19) Denissen, W.; Droesbeke, M.; Nicolaÿ, R.; Leibler, L.; Winne, J. M.; Du Prez, F. E. Chemical control of the viscoelastic properties of vinylogous urethane vitrimers. *Nat. Commun.* **2017**, *8*, 14857.

(20) Lessard, J. J.; Garcia, L. F.; Easterling, C. P.; Sims, M. B.; Bentz, K. C.; Arencibia, S.; Savin, D. A.; Sumerlin, B. S. Catalyst-Free Vitrimers from Vinyl Polymers. *Macromolecules* **2019**, *52*, 2105−2111.

(21) Denissen, W.; De Baere, I.; Van Paepegem, W.; Leibler, L.; Winne, J.; Du Prez, F. E. Vinylogous Urea Vitrimers and Their Application in Fiber Reinforced Composites. *Macromolecules* **2018**, *51*, 2054−2064.

(22) Guerre, M.; Taplan, C.; Nicolay, R.; Winne, J. M.; Du Prez, F. E. Fluorinated Vitrimer Elastomers with a Dual Temperature Response. *J. Am. Chem. Soc.* **2018**, *140*, 13272−13284.

(23) Ishibashi, J. S. A.; Kalow, J. A. Vitrimeric Silicone Elastomers Enabled by Dynamic Meldrum's Acid-Derived Cross-Links. *ACS Macro Lett.* **2018**, *7*, 482−486.

(24) Zheng, P.; McCarthy, T. J. A surprise from 1954: siloxane equilibration is a simple, robust, and obvious polymer self-healing mechanism. *J. Am. Chem. Soc.* **2012**, *134*, 2024−2027.

(25) Nishimura, Y.; Chung, J.; Muradyan, H.; Guan, Z. Silyl Ether as a Robust and Thermally Stable Dynamic Covalent Motif for Malleable Polymer Design. *J. Am. Chem. Soc.* **2017**, *139*, 14881−14884.

(26) Christensen, P. R.; Scheuermann, A. M.; Loeffler, K. E.; Helms, B. A. Closed-loop recycling of plastics enabled by dynamic covalent diketoenamine bonds. *Nat. Chem.* **2019**, *11*, 442−448.

(27) Lu, Y.-X.; Guan, Z. Olefin Metathesis for Effective Polymer Healing via Dynamic Exchange of Strong Carbon−Carbon Double Bonds. *J. Am. Chem. Soc.* **2012**, *134*, 14226−14231.

(28) Röttger, M.; Domenech, T.; van der Weegen, R.; Breuillac, A.; Nicolaÿ, R.; Leibler, L. High-performance vitrimers from commodity thermoplastics through dioxaborolane metathesis. *Science* **2017**, *356*, 62−65.

(29) Ricarte, R. G.; Tournilhac, F.; Leibler, L. Phase Separation and Self-Assembly in Vitrimers: Hierarchical Morphology of Molten and Semicrystalline Polyethylene/Dioxaborolane Maleimide Systems. *Macromolecules* **2019**, *52*, 432−443.

(30) Kloxin, C. J.; Scott, T. F.; Adzima, B. J.; Bowman, C. N. Covalent Adaptable Networks (CANs): A Unique Paradigm in Cross-Linked Polymers. *Macromolecules* **2010**, *43*, 2643−2653.

(31) He, C.; Christensen, P. R.; Seguin, T. J.; Dailing, E. A.; Wood, B. M.; Walde, R. K.; Persson, K. A.; Russell, T. P.; Helms, B. A. Conformational Entropy as a Means to Control the Behavior of Poly(diketoenamine) Vitrimers In and Out of Equilibrium. *Angew. Chem., Int. Ed.* **2019**, DOI: 10.1002/anie.201912223.

(32) Obadia, M. M.; Jourdain, A.; Cassagnau, P.; Montarnal, D.; Drockenmuller, E. Tuning the Viscosity Profile of Ionic Vitrimers Incorporating 1,2,3-Triazolium Cross-Links. *Adv. Funct. Mater.* **2017**, *27*, 1703258.

(33) Chen, X.; Li, L.; Torkelson, J. M. Recyclable polymer networks containing hydroxyurethane dynamic cross-links: Tuning morphology, cross-link density, and associated properties with chain extenders. *Polymer* **2019**, *178*, 121604.

(34) Chen, X.; Li, L.; Wei, T.; Torkelson, J. M. Reprocessable Polymer Networks Designed with Hydroxyurethane Dynamic Cross-links: Effect of Backbone Structure on Network Morphology, Phase Segregation, and Property Recovery. *Macromol. Chem. Phys.* **2019**, *220*, 1900083.

DOI: 10.1021/jacs.9b10360
J. Am. Chem. Soc. 2020, 142, 283−289

(35) Bates, C. M.; Bates, F. S. 50th Anniversary Perspective: Block Polymers—Pure Potential. *Macromolecules* **2017**, *50*, 3−22.
(36) Hill, M. R.; Carmean, R. N.; Sumerlin, B. S. Expanding the Scope of RAFT Polymerization: Recent Advances and New Horizons. *Macromolecules* **2015**, *48*, 5459−5469.
(37) Sims, M. B.; Lessard, J. J.; Bai, L.; Sumerlin, B. S. Functional Diversification of Polymethacrylates by Dynamic β-Ketoester Modification. *Macromolecules* **2018**, *51*, 6380−6386.
(38) Perrier, S.; Takolpuckdee, P.; Mars, C. A. Reversible Addition−Fragmentation Chain Transfer Polymerization: End Group Modification for Functionalized Polymers and Chain Transfer Agent Recovery. *Macromolecules* **2005**, *38*, 2033−2036.
(39) Flory, P. J. *Principles of Polymer Chemistry*; Cornell University Press: Ithaca, NY, 1953.
(40) Li, L. Q.; Chen, X.; Jin, K. L.; Torkelson, J. M. Vitrimers Designed Both To Strongly Suppress Creep and To Recover Original Cross-Link Density after Reprocessing: Quantitative Theory and Experiments. *Macromolecules* **2018**, *51*, 5537−5546.
(41) Noshay, A.; McGrath, J. E. *Block Copolymers: Overview and Critical Survey*; Elsevier Science, 2013.
(42) Goodwin, J. W.; Hughes, R. W. *Rheology for Chemists: An Introduction*; Royal Society of Chemistry, 2008.
(43) Edholm, O.; Blomberg, C. Stretched exponentials and barrier distributions. *Chem. Phys.* **2000**, *252*, 221−225.

DOI: 10.1021/jacs.9b10360
J. Am. Chem. Soc. 2020, 142, 283−289